

Effect of Oxygen Vacancies on Photocatalytic Efficiency of TiO₂ Nanotubes Aggregation

Feila Liu, Lu Lu, Peng Xiao,[†] Huichao He, Lei Qiao, and Yunhuai Zhang*

College of Chemistry and Chemical Engineering, Chongqing University, Chongqing 400030, China. *E-mail: xp2031@163.com

[†]College of Physics, Chongqing University, Chongqing 400030, China

Received November 30, 2011, Accepted April 2, 2012

Aggregation of titania nanotubes (TNTs) fabricated by hydrothermal method were calcined in air and dry nitrogen; Changes in morphology and crystallinity of the nanotubes were studied by means of TEM, EDX, and XPS. EDX patterns and XPS spectra proved that there were a certain densities of oxygen vacancies in TNTs annealed in N₂. The photocatalysis experiments revealed TNTs/N₂ possesses significantly higher photocatalytic efficiency than TNTs annealed in dry air to degrade methylene blue. The correlation between oxygen vacancies and photocatalytic property may be attributed to: 1) oxygen vacancies might have affected results on water molecules adsorption and increase of the hydroxyl concentration; and 2) oxygen vacancies resulted in some changes in electronic structure of TNTs/N₂ aggregation and Fermi level extends into the conducting band.

Key Words : Aggregation of TiO₂ nanotubes, Annealing treatment, Oxygen vacancies, Photocatalysis

Introduction

Transition metal oxide surfaces play an important role in a wide range of applications such as heterogeneous catalysis, photo-electrolysis, biocompatibility, and sanitary disinfection.^{1,2} TiO₂ is a typical transition metal oxide with an inherent photocatalytic activity. Among various oxide semiconductor photocatalysts, TiO₂ has the greatest potential due to nontoxicity, cheapness, strong oxidizing power, available in large amounts, environmental safety, and so on. Compared with any other form of titania for application in photocatalysis, titania nanotubes (TNTs) have attracted much attention because of their large specific surface area and favorable surface chemistry.^{3,4} Synthesis of 1D TiO₂ nanostructures may be achieved by various routes including template-assisted fabrication, anodic oxidation or anodization of titanium, and alkaline hydrothermal synthesis.⁵⁻⁹ TiO₂ nanotubes produced by hydrothermal synthesis possesses high specific surface area which can lead to much higher photocatalytic efficiency than the oriented structure and can be recycled efficiently.¹⁰ As a result, hydrothermal synthesis TiO₂ nanotubes aggregation have a great potential as photocatalyst for highly efficient photochemical applications.

It has been reported that surface defects including step edges, oxygen vacancies, line defects, impurities, and crystallographic shear planes dominate the electronic and photocatalytic properties of TiO₂ nanotubes.^{11,12} Among these defects, oxygen vacancies often dominate the electronic and chemical properties of transition metal oxide surfaces,¹³ can be obtained by ion sputtering,^{14,15} electron beam bombardment,¹⁶ thermal annealing in controlled gas,¹⁷ and low energy ultraviolet photons illumination.¹⁸ Annealing TiO₂ in various conditions can effectively alter the crystal structure and defect concentration.¹⁹⁻²² Hence, anneal in different gases is considered to be viable approach to narrow the band

gap and enhance the electrical conductivity of TNTs.

In this work, we report the photocatalytic activity of TNTs aggregation annealed in air and N₂ respectively. The experimental results revealed the photocatalytic efficiency of TNTs aggregation annealed in N₂ increased significantly than that of TNTs annealed in air. The influence of annealing gases on the defects of TNTs aggregation was studied by means of TEM, EDX, and XPS. The mechanism of oxygen vacancies on the photocatalytic properties of TNTs aggregation was also investigated.

Experimental Protocols

TNTs aggregation samples were prepared by a chemical process similar to that described by Kasuga *et al.*^{8,9} After the hydrothermal reaction, the obtained material was washed firstly by a 0.1 M HCl solution until the pH value reached *ca.* 3, and then by distilled water until the pH value of the rinsing solution reached *ca.* 6.5. After that, the samples were washed with ethanol, followed by centrifuging to separate the nanocatalyst from the suspension. The centrifuged samples were dried in a vacuum oven at 80 °C for 8 hours and then calcined at 450 °C in tube furnace, under a flow of dry air and N₂ for 3 hours, respectively. The resultant TNTs aggregation samples are hereinafter designated as: TNTs/air, for air-calcination, and TNTs/N₂, for nitrogen-calcination.

Methylene blue (C₁₆H₁₈ClN₃S·3H₂O) was employed as a model dye to evaluate the photocatalytic activity of the TNTs/air and TNTs/N₂. For each condition, 10 mg of catalyst was dispersed in 100 mL MB aqueous solution with an initial concentration of 4 × 10⁻⁶ mol/L. A 200 mL beaker containing the catalyst and solution was placed into a constant temperature water basin and a stirrer bar placed in the solution ensured full suspension of the catalyst throughout the experiment. The photocatalytic reaction was

conducted at a constant temperature 20 °C under UV light from a 30W mercury-vapour lamp at 365 nm positioned horizontally above the liquid surface. Each experiment conducted for 3 hours. The decomposition of MB was monitored by measuring the absorbance of aliquot solution using a spectrophotometer (Model: 722).

Transmission electron microscopy (TEM) analyses were conducted using a JEM-2010FEF electron microscope (JEOL, Tokyo, Japan), at 200 kV accelerating voltage. Elementary analysis were studied by energy dispersive X-ray detector (EDX, equip with SEM, Nova 400 Nano-SEM, FEI, Hillsboro, OR). Oxygen vacancies were measured by means of X-ray photoelectron spectroscopy (XPS, SSL-300 system, Surface Science Laboratory Inc., Sunnyvale, CA).

Results and Discussion

Morphology and Structure of TiO₂ Nanotubes. Figure 1 shows the SEM images of aggregation of TiO₂ nanotubes before annealing and after annealing in N₂ at 450 °C. The prepared nanotubes have an appearance of aggregation like wool balls. The TNTs aggregation after annealing possessed uniform diameter size of less than 1 μm. A single TiO₂ nanotube is fine with a short length, and it is apt to curl (Figure 1(b)). And hundreds of this kind of crooked nanotubes formed the structure of aggregation (Figure 1(a)). Subero *et al.* reported that particles held together by larger adhesive forces yield stronger agglomerates.³¹ This is largely related to the effect of surface energy on the mechanical properties of the agglomerate. The larger specific surface area and higher surface energy of TiO₂ nanotubes made the energy to be in an unstable state, and so the nanotubes became apt to form aggregation to achieve stability.

Figure 2 shows TEM images of the TiO₂ nanotubes before annealing (Figure 2(a), (b)), after annealing in air at 450 (Figure 2(c), (d)) and N₂ at 450 (Figure 2(e), (f)), respectively. The images of (a) and (b) indicated that the prepared nanotubes before annealing presented outer diameter of approximately 9 nm and inner diameter of approximately 4 nm, while (c), (d), (e) and (f) indicated that TiO₂ nanotubes presented thicker outer diameters of about 10 nm and thinner inner diameters of 2 nm after annealing. The tube walls of the nanotubes after annealing, which are approximately 4 nm, are much thicker than ones before annealing, which are

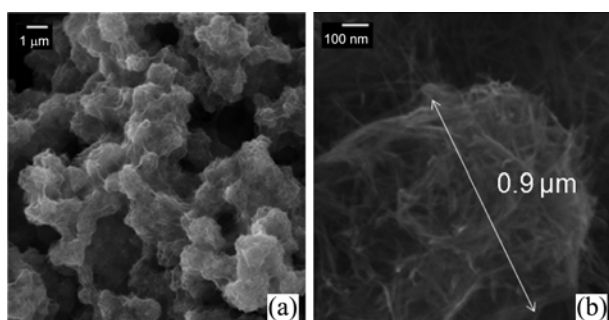


Figure 1. SEM images of aggregation of TiO₂ nanotubes.

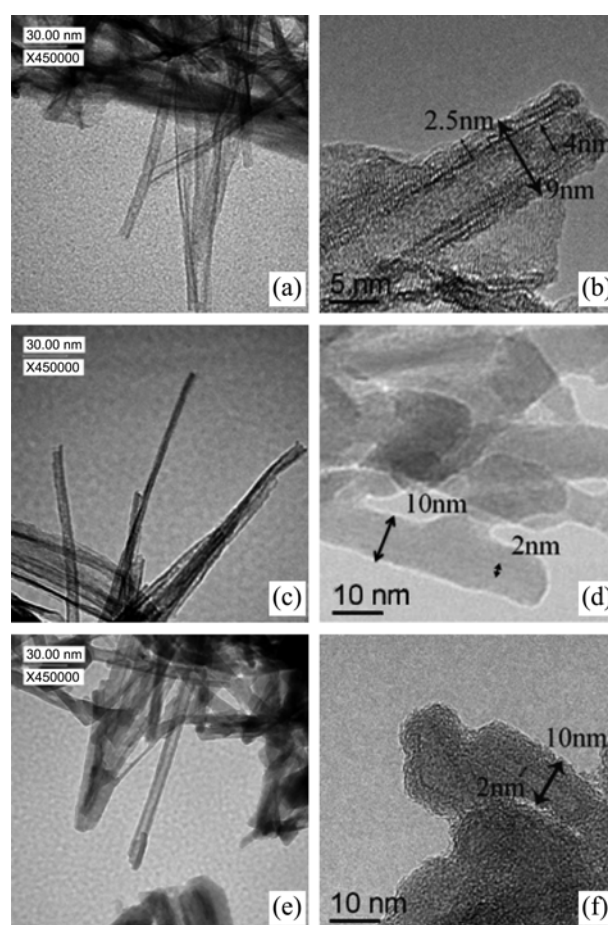


Figure 2. TEM images of TiO₂ nanotubes before annealing (a, b), after annealing in air (c, d) and in N₂ (e, f), respectively.

about 2.5 nm. And Figure 2(c), (d), (e) and (f) also revealed that the annealing gas atmospheres have almost no influence on the amorphous nature of TNTs.

Energy dispersive X-ray spectroscopy (EDX) analyses (Figure 3) revealed that the TNTs were mainly composed of titanium and oxygen, with trace amounts of carbon and other elements. Interestingly, the ratio of Ti and O is approximately 1:2 in the sample of TNTs/air; while the ratio of Ti and O is approximately 1:1.8 in TNTs/N₂. In order to accurately determine the degree of nonstoichiometry of TiO_{2-x}, further experiments with X-ray photoelectron spectroscopy (XPS) were introduced.

As shown in Figure 4, it was found that the two characteristic peaks of Ti2p_{1/2} was at ~465 eV and Ti2p_{3/2} was at ~459 eV in TNTs/air,^{23,35,36} but there was obvious shift to low binding energy in the two peak positions binding energy peaks of TNTs/N₂. This strongly suggested that Ti⁴⁺ had trends into transform to lower valence due to the loss of oxygen annealing in N₂. The full-width at half-maximum (fwhm) of the XPS peak corresponding to Ti⁴⁺ (the Ti2p_{3/2} spectra) is slightly affected by the annealing atmosphere. The Ti⁴⁺ peak varies from 1.02 to 2.05 for TNTs/air and TNTs/N₂, respectively. According to the literature,^{37,38} the obvious blue shift to low binding energy may be attributed to the charge effect. Part N atoms were introduced into the

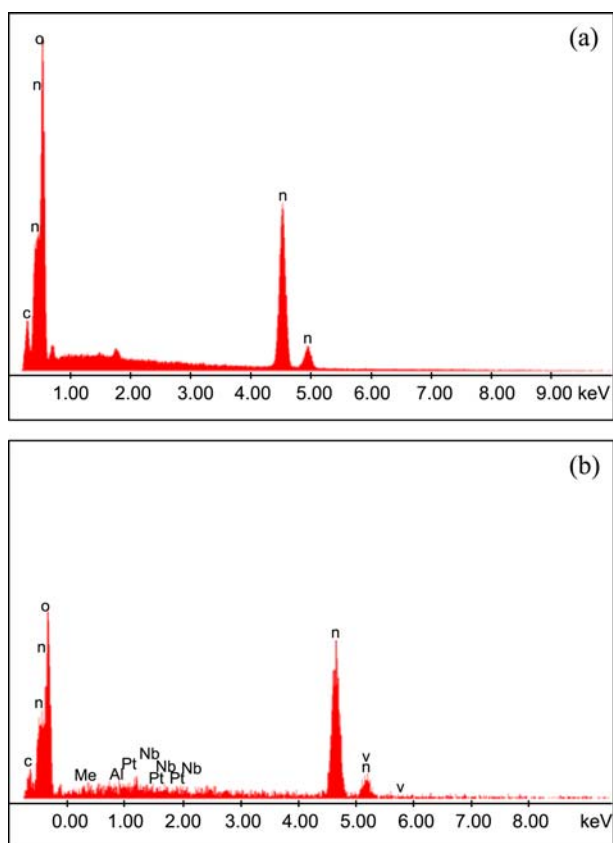


Figure 3. EDX patterns of TiO₂ nanotube annealed in air (a) and in N₂ (b) at 450 °C.

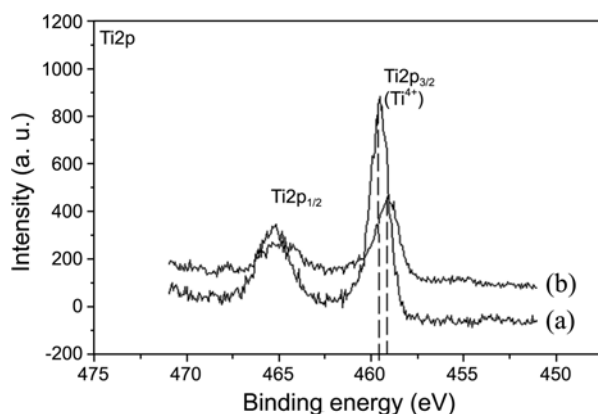


Figure 4. Ti2p XPS spectra of TiO₂ nanotubes annealed in air (a) and in N₂ (b) at 450 °C.

TiO₂ crystals and substituted for some of O atoms, the electronegativity of N is lower than that of O in the structure of O-Ti-N, and charges were transferred from N to Ti, which caused the increase of electron atmosphere density of Ti and the decrease of binding energy.

Table 1 is the element analysis of XPS spectra of TiO₂ nanotubes annealed in air and N₂, respectively. By comparison we found that the oxygen content of TNTs/air was higher than that of TNTs/N₂, which can be explained that the oxygen atoms were lost in the course of anneal in oxygen deficient condition in N₂, and oxygen vacancies appeared.

Table 1. The element analysis of XPS spectra of TiO₂ nanotubes annealed in air and N₂, respectively

Element	Atom content (%)	
	annealed in N ₂	annealed in air
Ti 2p	23.01	22.46
O 1s	60.30	62.72
C 1s	14.74	9.67
N 1s	0.48	0.28

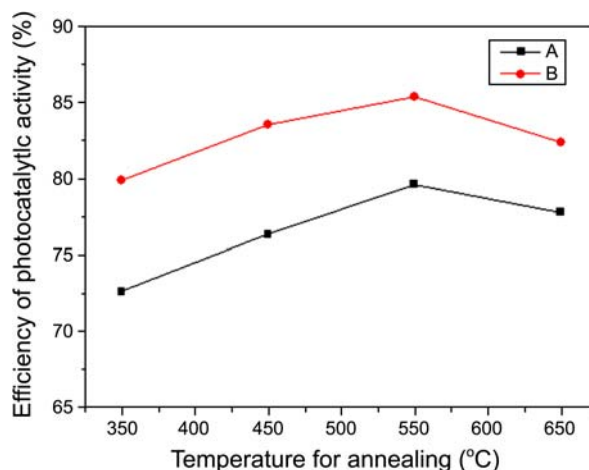


Figure 5. The efficiency of photocatalytic oxidation of methylene blue by TNTs/air aggregation (a) and TNTs/N₂ aggregation (b).

The content of carbon in TNTs/air was slightly lower, that mainly due to the generation of CO₂ in the process of annealing. In addition, the adsorption of N₂ on the surface of TNTs/ N₂ caused the content of N increased.³⁰

Photocatalytic Activity. The photocatalytic activity of TNTs/air aggregation and TNTs/N₂ aggregation was evaluated by photocatalytic oxidation of MB in air. Each experiment of photocatalytic oxidation lasted 3 hours. Figure 5 shows the efficiency of the photocatalytic oxidation of MB by TiO₂ nanotubes annealed in air and N₂ at 350 °C, 450 °C, 550 °C and 650 °C.

In Figure 5, obviously TNTs/N₂ aggregation possesses significantly higher photocatalytic efficiency than TNTs/air. This could be attributed to the formation of a certain densities of oxygen vacancies in TNTs/N₂ as discussed previously. The ideal TiO₂(110) surface has two characteristic surface sites: five-fold coordinated Ti⁴⁺ atoms and two-fold coordinated O²⁻ atoms. When the surface is slightly reduced by vacuum annealing, single oxygen vacancies (the most predominant surface defect) are formed.²⁵ It is generally accepted that O vacancies enhance the reactivity of the TiO₂ (110) surface.^{24,26-28} The correlation between oxygen vacancies and photocatalytic property of TNTs may be attributed to two aspects reasons. One is that oxygen vacancies might have affected results on water molecules adsorption and increase of the hydroxyl concentration. Schematic of the water molecules adsorption at the TiO₂ surface in TNTs/N₂ is shown in Figure 6. From this figure,

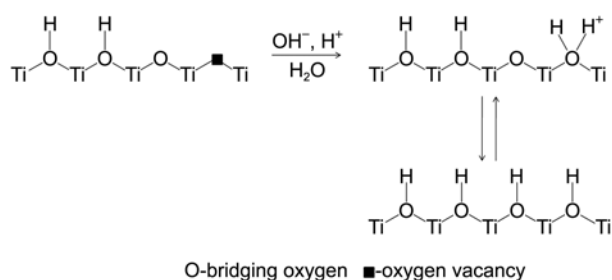
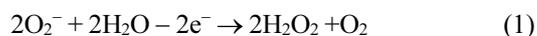


Figure 6. Schematic of the water molecules adsorption at the TiO₂ surface in TNTs/N₂.

we can see that once one O atom losing, Ti atoms presented at the TiO₂ surface become bonds to the hydroxyl groups due to water adsorption and dissociation. Correspondingly, the coordinated bridging O atoms at the surface become bonded to water-derived hydrogen. The dissociation of a water molecule at the surface thus results in two hydroxyl groups: one bonded to the previously coordinated Ti (the basic site) and the other formed by the bonding of a proton to the coordinated bridging O (the acidic site).²⁹

It was proved that O₂⁻ was generated by the combine of oxygen vacancies and O₂, which reduced the recombine of photo-generated electrons and holes.³³ As the active species, O₂⁻ surface states (valence-gap energy of 2.87 eV) can have reaction with the adsorbed water molecules as follows:



From the above reaction we can see that several small oxygen-containing molecules such as O₂⁻, H₂O₂ and •OH, highly reactive species are generated from the surrounding water by charge exchange between the valence band and conduction band. These radicals and peroxide ions are able to virtually oxidize all organic materials to CO₂ and H₂O. Hence, the existence of the O₂⁻ surface states was in favor of the separation of photo-generated carriers of TiO₂ surface. In addition, mainly due to the polarization of water, the surface band bending of TiO₂ increased after adsorbing a small amount of water molecules and the separation efficiency of photo-generated carriers was also enhanced. With the increase of the adsorbed water molecules on the surface of TiO₂, the holes transferred to the surface of TiO₂ and produced •OH with hydroxyl. The presence of •OH was beneficial to the photo oxidation, therefore, the higher hydroxyl content of TiO₂ surface had, the more •OH produced, which finally lead to the enhancement of the photocatalytic activity of TiO₂.³³

Another reason is that there are some changes in the electronic structure of TNTs/N₂ with oxygen vacancies, which lead to a change of the interaction between electrons. Heller et al considered that lattice defect can raise the Fermi level of TiO₂, correspondingly increase the height of the potential barriers that repel electrons from the surface, reduce the rate of recombination of electrons and holes.³⁴ Hou et al.³² studied the effect of oxygen vacancy in anatase

TiO₂ crystal on the optical property through using the plane waves ultrasoft pseudopotential technique, which was based on density functional theory. Compared with the pure anatase TiO₂ crystal, they found that the Fermi surface of the total density of states (TDOS) extended into the conducting band, which led to decrease of band gap and the Ti 3d state of the anatase crystal of TiO₂ at -6.097 eV showed new split peaks. According to the calculations, the band gap of the anatase crystal TiO₂ with oxygen vacancy reduced approximately by 0.176 eV. This result exerts an important influence on the optical property of TiO₂ crystal and is responsible for the large improvement in photocatalytic efficiency.

In our experiment, TNTs/N₂ aggregation possesses significantly higher photocatalytic efficiency than TNTs/air aggregation was observed. Annealing under a reductive environment, such as in nitrogen, the oxygen vacancies can be generated in the TiO₂ structure due to a partial oxygen loss. That in turn would results in more hydroxyl groups, which is discussed previously, and at the same time, would change the electron density and the electrical properties of the material. Consequently the two main reasons made a higher photocurrent density observed in TNTs aggregation annealed in nitrogen. In our future research, we will focus on which one is the predominant power in the two reasons.

Summaries

The experimental results revealed TNTs/N₂ aggregation possesses significantly higher photocatalytic efficiency than TNTs/air aggregation. This could be attributed to the formation of a certain densities of oxygen vacancies in TNTs/N₂ that proved by EDX patterns and Ti2p XPS spectra. The correlation between oxygen vacancies and photocatalytic property may be attributed to two reasons. One is oxygen vacancies might have affected results on water molecules adsorption and increase of the hydroxyl concentration. And another reason is oxygen vacancies resulted in some changes in electronic structure of TNTs/N₂ aggregation and Fermi level extends into the conducting band.

Acknowledgments. This research was financed by the Scientific & Research Project of Scientific Committee of Chongqing under Project No. CSTC, 2009BB4047; Chongqing University Postgraduates Science & Innovation Fund under Project No. CDJXS10 22 11 42; Innovative Talent Training Project, the Third Stage of "211 project", Chongqing University (Grant No. S-09103).

References

1. Kasemo, B.; Gold, J. *Adv. Dent. Res.* **1999**, *13*, 8.
2. Heller, A. *Acc. Chem. Res.* **1995**, *28*, 503.
3. Gong, D.; Grimes, C. A.; Varghese, O. K.; Hu, W.; Singh, R. S.; Chen, Z.; Dickey, E. C. *J. Mater. Res.* **2001**, *16*, 3331.
4. Ghicov, A.; Suchiya, H.; Macak, J. M.; Schmuki, P. *Electrochem. Commun.* **2005**, *7*, 505.
5. Sander, M. S.; Cote, M. J.; Gu, W.; Kile, B. M.; Tripp, C. P. *Adv.*

- Mater.* **2004**, *16*, 2052.
6. Michailowski, A.; AlMawlawi, D.; Cheng, G. S.; Moskovits, M. *Chem. Phys. Lett.* **2001**, *349*, 1.
 7. Macak, J. M.; Tsuchiya, H.; Schmuki, P. *Angew. Chem. Int. Ed.* **2005**, *44*, 2100.
 8. Kasuga, T.; Hiramatsu, M.; Hoson, A.; Sekino, T.; Niihara, K. *Langmuir* **1998**, *14*, 3160.
 9. Kasuga, T.; Hiramatsu, M.; Hoson, A.; Sekino, T.; Niihara, K. *Adv. Mater.* **1999**, *11*, 1307.
 10. Lu, L.; Zhang, Y. H.; Xiao, P.; Zhang, X. N.; Yang, Y. N. *Environ. Sci. Technol.* **2010**, *27*, 281.
 11. Zhang, Y. H.; Xiao, P.; Zhou, X. Y.; Liu, D.; Garcia, B. B.; Cao, G. *Z. J. Mater. Chem.* **2009**, *19*, 948.
 12. Henrich, V. E.; Cox, P. A. *The Surface Science of Metal Oxides*; Cambridge University Press: Cambridge, 1994.
 13. Hou, Q.; Zhang, Y.; Zhang, T. *Acta Optica Sinica* **2008**, *28*, 1347.
 14. Petigny, S.; Domenichini, B.; Mostefa-sba, H.; Lesniewska, E.; Steinbrunn, A.; Bourgeois, S. *Appl. Surf. Sci.* **1999**, *142*, 114.
 15. Schaub, R.; Wahlstrom, E.; Anders, R.; Lsgaard, E.; Stensgaard, I.; Besenbacher, F. *Science* **2003**, *299*, 17.
 16. Wang, L. Q.; Baer, D. R.; Engelhard, M. H. *Surf. Sci.* **1994**, *320*, 295.
 17. Norenberg, H.; Dinelli, F.; Briggs, G. A. D. *Surf. Sci.* **2000**, *446*, L83.
 18. Wang, R.; Hashimoto, K.; Fujishima, A.; Chikuni, M.; Kojima, E.; Kitamura, A.; Shimohigoshi, M.; Watanabe, T. *Nature* **1997**, *388*, 431.
 19. Noworyta, K.; Augustynski, J. *Solid-State Lett.* **2004**, *7*, E31.
 20. Mor, G. K.; Varghese, O. K.; Paulose, M.; Shankar, K.; Grimes, C. A. *Sol. Energy Mater. Sol. Cells* **2006**, *90*, 2011.
 21. Ghicov, A.; Macak, J. M.; Tsuchiya, H.; Kunze, J.; Haeublein, V.; Frey, L.; Schmuki, P. *Nano. Lett.* **2006**, *6*, 1080.
 22. Vitiello, R. P.; Macak, J. M.; Ghicov, A.; Tsuchiya, H. L.; Dick, F. P.; Schmuki, P. *Electrochem. Commun.* **2006**, *8*, 544.
 23. Gopel, W.; Anderson, J. A.; Frankel, D.; Jaehnig, M.; Phillips, K.; Schafer, J. A.; Rocker, G. *Surf. Sci.* **1984**, *139*, 333.
 24. Henderson, M. A.; Epling, W. S.; Perkins, C. L.; Peden, C. H. F. *J. Phys. Chem. B* **1999**, *103*, 5328.
 25. Diebold, U.; Lehman, J.; Mahmoud, T.; Kuhn, M.; Leonardelli, G.; Hebenstreit, W.; Schmid, M.; Varga, P. *Surf. Sci.* **1998**, *411*, 137.
 26. Gopel, W.; Rocker, G.; Feierabend, R. *Phys. Rev. B* **1983**, *28*, 3427.
 27. Linsebigler, A.; Lu, G.; Yates, J. T. J., Jr. *Chem. Phys.* **1995**, *103*, 438.
 28. Schaub, R.; Thostrup, P.; Lopez, N.; Laegsgaard, E.; Stensgaard, I.; Norskov, J. K.; Besenbacher, F. *Phys. Rev. Lett.* **2001**, *87*, 266104.
 29. Guillemot, F. M.; Porte, C.; Labrugere, C.; Baquey, C. *J. Col. Int. Sci.* **2002**, *255*, 75.
 30. X, P. *Thesis for the Doctorate of Chongqing University* **2008**, 44.
 31. Subero, J.; Ning, Z.; Ghadiei, M.; Thornton, C. *Powder Technol.* **1999**, *105*, 66.
 32. Hou, Q. Y.; Zhang, Y.; Zhang, T. *Acta Optica Sinica.* **2008**, *28*, 1347.
 33. Li, X. Q.; Qiao, G. J.; Chen, J. *Journal of the Chinese Ceramic Society* **2006**, *34*, 1466.
 34. Heller, A.; Degani, Y.; Johnson, D. W.; Gallagher, P. K.; Gallagher, Jr. *Phys. Chem.* **1987**, *91*, 5987.
 35. Zhang, Y. H.; Xiao, P.; Zhou, X. Y.; Liu, D. W.; Cao, G. Z. *J. Mater. Chem.* **2009**, *19*, 948.
 36. Liu, D. W.; Zhang, Y. H.; Xiao, P.; Garcia, B. B.; Zhang, Q. F.; Zhou, X. Y.; Cao, G. Z. *Electrochim. Acta* **2009**, *54*, 6816.
 37. Cong, Y.; Xiao, L.; Zhang, J. *Res. Chem. Intermed.* **2006**, *32*, 717.
 38. Burda, C.; Lou, Y.; Chen, X. *Nano Lett.* **2003**, *3*, 1049.
-